

Calculation of thallium hyperfine anomaly

E. A. Konovalova¹, M. G. Kozlov^{1,2}, Yu. A. Demidov^{1,2}, and A. E. Barzakh¹

¹ *Petersburg Nuclear Physics Institute, Gatchina 188300, Russia and*

² *St. Petersburg Electrotechnical University "LETI", Prof. Popov Str. 5, 197376 St. Petersburg*

(Dated: November 9, 2018)

We suggest a method to calculate hyperfine anomaly for many-electron atoms and ions. At first, we tested this method by calculating hyperfine anomaly for hydrogen-like thallium ion and obtained fairly good agreement with analytical expressions. Then we did calculations for the neutral thallium and tested an assumption, that the ratio between the anomalies for s and $p_{1/2}$ states is the same for these two systems. Finally, we come up with recommendations about preferable atomic states for the precision measurements of the nuclear g factors.

I. INTRODUCTION

In recent years, the precision achieved in resonant ionization spectroscopy experiments coupled with advances in atomic theory has enabled new atomic physics based tests of nuclear models. Understanding the occurrence of shape coexistence in atomic nuclei is one of them. This phenomenon is associated with existence of both the near-spherical and deformed structures of nuclei for neutron-deficient isotopes near $Z = 82$ closed shell. The measurements of hyperfine constants and isotope shifts are highly sensitive to the changes of nuclear charge and magnetic radii because they depend on the behavior of the electron wave function near the nucleus. The hyperfine structure (HFS) measurements can serve as very useful tool for understanding of shape coexistence phenomena in atomic nuclei.

Magnetic hyperfine constants A are usually assumed to be proportional to the nuclear magnetic moments. However, this is true only for the point-like nucleus. For the finite nucleus we need to take into account (i) distribution of the magnetization inside the nucleus and (ii) dependence of the electron wave function on the nuclear charge radius. Former correction is called magnetic (Bohr–Weisskopf [1]) and the latter is called charge correction (Breit-Rosenthal[2, 3]). Together these corrections are known as hyperfine anomaly [4]. Below we discuss how to calculate hyperfine anomaly for many-electron atoms with available atomic packages. We use thallium atom as reference system for our calculations, because for this atom there are comprehensive experimental data [5–9] and many theoretical calculations [4, 10–13].

Shabaev [4] and Shabaev et al. [10] found analytical expressions for the hyperfine anomaly for H-like thallium ion. For the neutral thallium there is numerical calculation by Mårtesson-Pendrill [11]. Experimentally HFS anomaly is studied much better for neutral Tl than for respective H-like ion. In the work [14] it has been suggested, that the ratio between the anomalies for s and $p_{1/2}$ states remains constant for these two systems. Here we try to test this assumption.

We use atomic package [15], which is based on the original Dirac-Hartree-Fock code [16]. This package is often used to calculate different atomic properties including

hyperfine structure constants of Tl [12, 13], Yb [17], Mg [18], and Pb [19].

II. THEORY AND METHODS

A four component Dirac wavefunction of an electron in a spherically symmetric atomic potential can be written as [16]:

$$\psi_{n,\kappa,m}(\mathbf{r}) = \frac{1}{r} \begin{pmatrix} P_{n,\kappa}(r)\Omega_{\kappa,m}(\omega) \\ -iQ_{n,\kappa}(r)\Omega_{-\kappa,m}(\omega) \end{pmatrix}, \quad (1)$$

where relativistic quantum number $\kappa = (l-j)(2j+1)$ and $\Omega_{-\kappa,m}$ is spherical spinor. In these notations the radial integral for the magnetic hyperfine constant for the point-like nuclear magnetic moment in the origin has the form:

$$I_{n',\kappa',n,\kappa} = \int_0^\infty (P_{n',\kappa'}Q_{n,\kappa} + Q_{n',\kappa'}P_{n,\kappa}) \frac{dr}{r^2}. \quad (2)$$

Magnetization of the nucleus is formed by the spin polarization of nucleons and by the orbital motion of protons. Bohr and Weisskopf [1] noted that if nuclear magnetization is localized at the spherical nuclear surface, then the spin contribution vanishes inside the nucleus, while the orbital one grows linearly from the center. Similar linear growth corresponds to the uniform spin distribution inside the nucleus. Radial integral inside the nucleus of radius R_N for this case has the form [11]:

$$I_{n',\kappa',n,\kappa}^{\text{nuc}} = \int_0^{R_N} (P_{n',\kappa'}Q_{n,\kappa} + Q_{n',\kappa'}P_{n,\kappa}) \frac{r dr}{R_N^3}. \quad (3)$$

Outside the nucleus expression (2) still holds.

In our package we use the model of the uniformly charged ball and inside the nucleus we use Taylor expansion for the radial functions P and Q :

$$P_{n,\kappa}(r)|_{r \leq R_N} = r^{|\kappa|} \sum_{k=0}^M P_{n,\kappa,k} x^k, \quad x = \frac{r}{R_N}. \quad (4)$$

With the help of this expansion we can calculate integral

(3) and nuclear contribution to integral (2):

$$I_{n',\mathcal{Z}',n,\mathcal{Z}}^{\text{nuc}} = R_N^{|\mathcal{Z}'|+|\mathcal{Z}|-1} \times \sum_{m=0}^M \sum_{k=0}^m \frac{P_{n',\mathcal{Z}',k} Q_{n,\mathcal{Z},m-k} + Q_{n',\mathcal{Z}',k} P_{n,\mathcal{Z},m-k}}{|\mathcal{Z}'| + |\mathcal{Z}| + m + 2}, \quad (5)$$

$$I_{n',\mathcal{Z}',n,\mathcal{Z}}^{\text{nuc},0} = R_N^{|\mathcal{Z}'|+|\mathcal{Z}|-1} \times \sum_{m=0}^M \sum_{k=0}^m \frac{P_{n',\mathcal{Z}',k} Q_{n,\mathcal{Z},m-k} + Q_{n',\mathcal{Z}',k} P_{n,\mathcal{Z},m-k}}{|\mathcal{Z}'| + |\mathcal{Z}| + m - 1}. \quad (6)$$

Using expression (6) for two different nuclear radii we can calculate charge correction to atomic HFS, while using expression (5) we simultaneously account for charge

and magnetic corrections.

In order to disentangle these two corrections we introduce magnetic radius of the nucleus R_M . We assume that expressions (5) and (6) hold for $r \leq R_M$ and $r > R_M$ respectively. For the volume distribution of magnetization these two expressions should match each other at $r = R_M$. However, for the surface distribution there may be a gap between them. We multiply (5) by a factor $(1 - C_S)$ to account for this gap. Then $C_S = 0$ gives smooth behavior at the surface and $C_S = 1$ corresponds to the zero contribution of the volume inside the nucleus. Our final expression for the radial integral inside the nucleus combines integrand from Eq. (3) for $r \leq R_M$ with the integrand from Eq. (2) for $R_M < r \leq R_N$:

$$I_{n',\mathcal{Z}',n,\mathcal{Z}}^{\text{nuc}}(R_N, R_M) = (1 - C_S) I_{n',\mathcal{Z}',n,\mathcal{Z}}^{\text{nuc}}(R_M) + \left(I_{n',\mathcal{Z}',n,\mathcal{Z}}^{\text{nuc},0}(R_N) - I_{n',\mathcal{Z}',n,\mathcal{Z}}^{\text{nuc},0}(R_M) \right), \quad (7)$$

$$I_{n',\mathcal{Z}',n,\mathcal{Z}}^{\text{nuc}}(R_M) = R_M^{|\mathcal{Z}'|+|\mathcal{Z}|-1} \sum_{m=0}^M \sum_{k=0}^m \frac{P_{n',\mathcal{Z}',k} Q_{n,\mathcal{Z},m-k} + Q_{n',\mathcal{Z}',k} P_{n,\mathcal{Z},m-k}}{|\mathcal{Z}'| + |\mathcal{Z}| + m + 2} \left(\frac{R_M}{R_N} \right)^m, \quad (8)$$

$$I_{n',\mathcal{Z}',n,\mathcal{Z}}^{\text{nuc},0}(R_M) = R_M^{|\mathcal{Z}'|+|\mathcal{Z}|-1} \sum_{m=0}^M \sum_{k=0}^m \frac{P_{n',\mathcal{Z}',k} Q_{n,\mathcal{Z},m-k} + Q_{n',\mathcal{Z}',k} P_{n,\mathcal{Z},m-k}}{|\mathcal{Z}'| + |\mathcal{Z}| + m - 1} \left(\frac{R_M}{R_N} \right)^m. \quad (9)$$

Equation (7) describes several limiting cases. Taking $R_M = 0$ we return to the point magnetic dipole model. For $R_M = R_N$ and $C_S = 0$ we get model (5). Finally, for $R_M = R_N$ and $C_S = 1$ we completely eliminate nuclear contribution to the radial integral.

A. Isotope effect for magnetic HFS

Suppose we want to compare hyperfine constants A_1 and A_2 for two isotopes with nuclear g factors $g_I^{(1)}$ and $g_I^{(2)}$, nuclear charge radii $R_N^{(1)}$ and $R_N^{(2)}$, and magnetic radii $R_M^{(1)}$ and $R_M^{(2)}$. We can write:

$$\frac{A_1}{A_2} = \frac{g_I^{(1)}}{g_I^{(2)}} \left(1 - \lambda^C \frac{R_N^{(1)} - R_N^{(2)}}{R_N^{(1)} + R_N^{(2)}} - \lambda^M \frac{R_M^{(1)} - R_M^{(2)}}{R_M^{(1)} + R_M^{(2)}} \right). \quad (10)$$

The anomaly then has the following form:

$${}^1\Delta^2 \equiv \frac{g_I^{(2)} A_1}{g_I^{(1)} A_2} - 1 = - \left(\lambda^C \frac{R_N^{(1)} - R_N^{(2)}}{R_N^{(1)} + R_N^{(2)}} + \lambda^M \frac{R_M^{(1)} - R_M^{(2)}}{R_M^{(1)} + R_M^{(2)}} \right). \quad (11)$$

With the help of the method described above we can calculate hyperfine constant for several values of R_N and

R_M . By solving above equations for several radii, we can find λ^C and λ^M and calculate the anomaly for the isotopes of interest. Below we will see that parameters λ^C and λ^M themselves depend on the radii R_N and R_M . Therefore it is better to use parameters b_N and b_M defined below (see Eq. (18)).

B. Hydrogen-like ions

It is generally accepted that the observed hyperfine constant $A(R_N, R_M)$ of a one-electron ion can be written in the following form:

$$A(R_N, R_M) = A_0 (1 - \delta(R_N))(1 - \epsilon(R_M)). \quad (12)$$

Here $A_0 \equiv A(0, 0)$ is the factor, which is independent of nuclear radii and $\delta(R_N)$ and $\epsilon(R_M)$ are the nuclear charge distribution and magnetic distribution corrections respectively. For a given Z and electron state, they can be written as:

$$\delta(R_N) = b_N R_N^{2\gamma-1}, \quad \epsilon(R_M) = b_M R_M^{2\gamma-1}, \quad (13)$$

where b_N and b_M are factors, which are independent of nuclear radii, $\gamma = \sqrt{\mathcal{Z}^2 - (\alpha Z)^2}$, and α is the fine structure constant. The expression for A_0 was obtained in the analytical form as [4]:

$$A_0 = \frac{\alpha(\alpha Z)^3 g_I}{j(j+1)} \frac{m}{m_p} \frac{\mathcal{Z}(2\mathcal{Z}(\gamma + n_r) - N)}{N^4 \gamma(4\gamma^2 - 1)} m c^2. \quad (14)$$

Here m and m_p are electron and proton masses, $g_I = \mu/I$ is nuclear g factor, j is the total electron angular momentum, $N = \sqrt{n_r^2 + 2n_r\gamma + \varkappa^2}$, n_r is radial quantum number.

It follows from Eqs. (12) and (13), that if we calculate HFS constant numerically for different R_N and R_M , we should get following dependence on the radii:

$$A(R_N, R_M) = A_0(1 - b_N R_N^{2\gamma-1})(1 - b_M R_M^{2\gamma-1}). \quad (15)$$

This expression defines the dependence of parameters λ^C and λ^M from (10) on the radii R_N and R_M . For example, from one hand, we have:

$$\frac{A(R_N + \rho, R_M)}{A(R_N - \rho, R_M)} = 1 - \lambda^C(R_N) \frac{\rho}{R_N}. \quad (16)$$

From the other hand:

$$\frac{A(R_N + \rho, R_M)}{A(R_N - \rho, R_M)} = 1 + 2\rho \frac{\partial A(R_N, R_M)/\partial R_N}{A(R_N, R_M)}. \quad (17)$$

Then, from Eq. (16) we get:

$$\begin{aligned} \lambda^C(R_N) &\approx \frac{2(2\gamma - 1)b_N R_N^{2\gamma-1}}{1 - b_N R_N^{2\gamma-1}} \\ &\approx 2(2\gamma - 1)b_N R_N^{2\gamma-1}. \end{aligned} \quad (18)$$

Similar expressions can be obtained for $\lambda^M(R_M)$.

For the point-like magnetic dipole approximation ($R_M = 0$) the magnetic correction ϵ is equal 0, and the hyperfine constant can be fitted by the function:

$$A(R_N, 0) = A_0(1 - b_N R_N^{2\gamma-1}). \quad (19)$$

For the uniform distribution of the charge and magnetic moment with $R_N = R_M$ we get:

$$A(R_N, R_N) = A_0(1 - (b_N + b_M)R_N^{2\gamma-1}) \quad (20)$$

C. Many-electron atoms

Since the one-electron radial integrals are defined, we can calculate atomic HFS using many-electron wave functions and account for electronic correlations as described in Ref. [12]. Using Eqs. (7 – 9) we can calculate atomic HFS constants for arbitrary radii R_N and R_M with the only constraint that $R_N \geq R_M$. We can do configuration interaction calculations with the frozen core and few valence electrons. Then we can add core-valence correlation corrections with the help of the many-body perturbation theory. On this stage we substitute valence radial integrals with the effective ones, which account for the spin polarization of the core. The latter are obtained by solving random-phase approximation (RPA) equations.

Effective radial integrals may have significantly different dependence on the parameters of the nucleus, than initial “bare” integrals. This is particularly true for the

orbitals with high angular momentum. Because of the centrifugal barrier these orbitals do not penetrate inside the nucleus and bare radial integrals do not depend on the nuclear size. On the other hand, spin-polarization of the core always include polarization of the core s and $p_{1/2}$ shells. Because of that all effective radial integrals are sensitive to the nuclear charge and magnetic distributions.

In general, we can divide all correlation corrections in two classes: corrections, which mix orbitals within one partial wave, and the ones which mix different partial waves. For example, the self-energy type corrections belong to the first class. They mix core and valence orbitals of the same symmetry and can significantly change the orbital density at the origin. Therefore, these corrections change the size of the HFS matrix elements. On the other hand, all orbitals of the same symmetry have practically the same sensitivity to the nuclear distributions. Thus, such correlation corrections do not affect parameters b_N and b_M and the HFS anomaly (11). RPA corrections belong to the second class, which significantly contribute to the HFS anomaly.

III. RESULTS AND DISCUSSION

A. HFS anomaly for H-like thallium ion

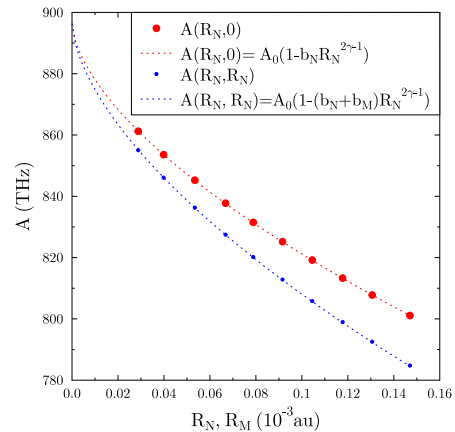


FIG. 1: The dependence of the HFS constant $A(R_N, R_M)$ for the ground state of H-like Tl ion from nuclear charge and magnetic radii. Dots and circles correspond to the computed values. Dashed lines correspond to the fits by Eqs. (19) and (20).

In this section we calculate HFS constants of the $1s$, $2s$, and $2p_{1/2}$ states of Tl^{80+} for different radii R_N and R_M and compare our results with analytical expressions from Ref. [4]. Figure 1 shows the dependence of the hyperfine

constant $A(1s)$ on the radii R_N and R_M . We see very good agreement with Eqs. (19) and (20).

TABLE I: Compilation of the fitting parameters for HFS of H-like Tl ion: A_0 is HFS constant for point-like nucleus, δ and ϵ are the nuclear charge and magnetization distribution corrections parametrized by b_N and b_M coefficients respectively. We use g factor $g_I = 3.27640$. Corrections δ and ϵ for ^{203}Tl are calculated for $R_N = R_M = 0.1306 \times 10^{-3}$ au.

		1s	2s	$2p_{1/2}$
A_0 (THz)	fit.	896.4	144.9	45.0
	Eq. (14)	895.7	144.8	45.0
b_N	fit.	0.3441	0.3671	0.0960
	δ for $^{203}\text{Tl}^{80+}$	fit.	0.0988	0.105
Ref. [10]		0.0988	–	–
b_M	fit.	0.0599	0.0638	0.0176
	ϵ for $^{203}\text{Tl}^{80+}$	fit.	0.0172	0.0183
Ref. [10]		0.0179	–	–

Table I summarizes our results for H-like Tl ion. We see perfect agreement of the calculated and analytical values of A_0 for all three states. Charge and magnetic corrections δ and ϵ were calculated in Ref. [10] for the 1s state of the isotope ^{203}Tl . These analytical values are also in good agreement with our numerical results.

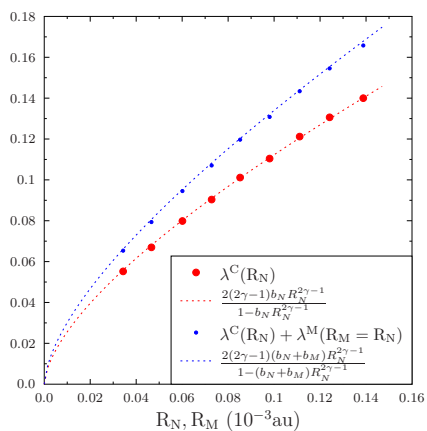


FIG. 2: Dependence of the parameters $\lambda^C(R_N)$ and $\lambda^M(R_M)$ (see Eq. (10)) on the charge and magnetic radii of the nucleus for the ground state of H-like Tl ion. Computed values represented by points. The curves correspond to the fits with Eq. (18).

Figure 2 shows how parameters λ for the 1s state depend on the radii R_N and R_M . On one hand, we see perfect agreement with the analytical expression (18). On the other hand, it means that these parameters strongly depend on the nuclear size. Because of that they can not be treated as constant even for the isotopes with similar radii. Therefore it is better to use parameters b_N and b_M defined by Eq. (15).

According to our calculations (see Table I) the ratios of the parameters b_N and b_M for 1s and 2s states are close to unity: $\frac{b_N(1s)}{b_N(2s)} = 0.937$ and $\frac{b_M(1s)}{b_M(2s)} = 0.939$. This is expected, as wave functions of the same symmetry should be proportional to each other inside the nucleus. Similar ratios for 1s and $2p_{1/2}$ states are $\frac{b_N(1s)}{b_N(2p_{1/2})} = 3.58$ and $\frac{b_M(1s)}{b_M(2p_{1/2})} = 3.40$. Again, one can expect that these ratios only weakly depend on the principle quantum numbers.

B. HFS anomaly of neutral thallium atom

The ground configuration of the neutral thallium is $[1s^2 \dots 6s^2]6p$ and the ground multiplet includes two levels, $6p_{1/2}$ and $6p_{3/2}$. The lowest level of the opposite parity is 7s. Most of the experiments and calculations of the HFS in neutral thallium deal with these three levels. If we treat thallium as a one-electron system with the frozen core $[1s^2 \dots 6s^2]$, we can do calculation using Dirac-Hartree-Fock (DHF) method. In this case the dependence of the HFS constants on the nuclear radii is similar to the one-electron ion.

TABLE II: Compilation of the fitting parameters for HFS of neutral Tl atom: A_0 is HFS constant for point-like nucleus, δ and ϵ are the nuclear charge and magnetization distribution corrections parametrized by b_N and b_M coefficients respectively. We use g factor $g_I = 3.27640$. Corrections δ and ϵ for ^{203}Tl are calculated for $R_N = R_M = 0.1306 \times 10^{-3}$ au. Calculations are done within DHF and DHF+RPA approximations.

	DHF		DHF+RPA			
	$6p_{1/2}$	7s	$6p_{3/2}$	$6p_{1/2}$	7s	$6p_{3/2}$
A_0 (GHz)	18.308	8.942	1.315	22.960	12.586	-2.423
b_N	0.1054	0.3709	0	0.1352	0.3517	0.5302
δ for ^{203}Tl	0.0303	0.1064	0	0.0388	0.1009	0.1522
b_M	0.0195	0.0621	0	0.0250	0.0643	0.0989
ϵ for ^{203}Tl	0.0056	0.0178	0	0.0072	0.0185	0.0284

In DHF approximation the HFS constant $A(6p_{3/2}) = 1.30$ GHz is very small and practically does not depend on R_N and R_M (see Table II). At the same time, the HFS constants $A(6p_{1/2})$ and $A(7s)$ are well described by Eqs. (19, 20) (see Fig. 3). According to our calculations, the ratios between coefficients b_N and b_M for s and $p_{1/2}$ waves are close to the respective ratios in H-like ion. For example, the ratios of these constants for 1s state of the ion and 7s state of the neutral atom are $\frac{b_N(1s)}{b_N(7s)} = 0.928$ and $\frac{b_M(1s)}{b_M(7s)} = 0.965$. This result is compatible with assertion that the hyperfine anomaly measured for the s states in Rb is independent of the principal quantum number [20]. Atomic ratios for 7s and $6p_{1/2}$ are: $\frac{b_N(7s)}{b_N(6p_{1/2})} = 3.52$ and $\frac{b_M(7s)}{b_M(6p_{1/2})} = 3.18$, while for the H-like ion we had 3.58 and 3.40 respectively.

Situation changes when we include spin-polarization of the core via RPA corrections. These corrections mix

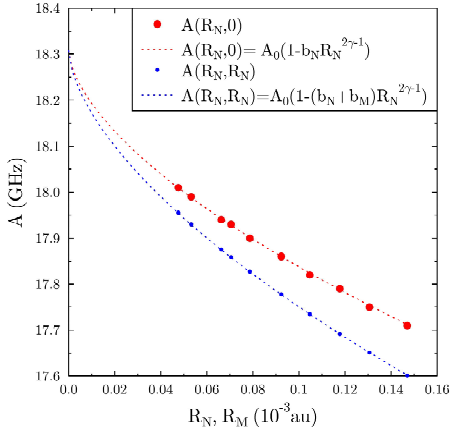


FIG. 3: The dependence of the HFS constant $A(R_N, R_M)$ for the ground state of neutral Tl ion from nuclear charge and magnetic radii. Dots and circles correspond to the computed values within Dirac-Hartree-Fock method. Dashed lines correspond to the fits by Eqs. (19) and (20).

partial waves and the state $6p_{3/2}$ partly acquire s and $p_{1/2}$ character. This leads to significant change of the size and even the sign of the constant $A(6p_{3/2})$. At the same time this constant becomes very sensitive to the distributions of charge and magnetic moment inside the nucleus. RPA corrections for the $7s$ and $6p_{1/2}$ states are smaller than for $6p_{3/2}$, but also significant. They lead to effective mixing of the s and p waves. Because of that the ratios of the respective coefficients decrease a little, but are still much bigger than unity:

$$\frac{b_N(7s)}{b_N(6p_{1/2})} = 2.60, \quad \frac{b_M(7s)}{b_M(6p_{1/2})} = 2.57. \quad (21)$$

We conclude that in the DHF+RPA approximation, the anomaly for the $7s$ state is still significantly stronger, than for $6p_{1/2}$ state. The anomaly for the $6p_{3/2}$, on the contrary, becomes the largest. This conclusion holds when we include more correlation corrections, as it was done in [12].

Using experimentally measured value for HFS anomaly (10) for the ground state $6p_{1/2}$ of the thallium two stable isotopes $^{205}\Delta^{203}(6p_{1/2}) = -1.036(3) \times 10^{-4}$ [5], and the ratios (21) calculated here, we can obtain corresponding value for the $7s$ state within $R_N = R_M$ approximation: $^{205}\Delta^{203}(7s) = -2.7 \times 10^{-4}$. This value is significantly lower, than experimental value $-4.7(1.5) \times 10^{-4}$ obtained in Ref. [6].

IV. NUCLEAR MAGNETIZATION

In this section we discuss how much we can say about nuclear magnetization from the atomic hyperfine struc-

TABLE III: Magnetic HFS constants (MHz) for ^{203}Tl calculated for $R_N = 0.1306 \times 10^{-3}$ a.u. and different values of R_M and C_S .

R_M/R_N	0	1	1	0.9	0.8
C_S	0	1	0	0.345	0.805
DHF					
$A(6p_{1/2})$	17754.26	17590.89	17650.92	17650.83	17650.91
$A(6p_{3/2})$	1314.50	1314.50	1314.50	1314.50	1314.50
$A(7s_{1/2})$	7990.45	7732.08	7826.81	7826.64	7826.71
$A(7p_{1/2})$	1970.07	1951.94	1958.60	1958.59	1958.60
$A(7p_{3/2})$	188.10	188.10	188.10	188.10	188.10
DHF+RPA					
$A(6p_{1/2})$	22068.38	21806.94	21903.16	21903.01	21903.16
$A(6p_{3/2})$	-2057.68	-1949.05	-1989.17	-1989.12	-1989.20
$A(7s_{1/2})$	11322.86	10957.33	11091.66	11091.44	11091.60
$A(7p_{1/2})$	2029.95	2014.27	2020.03	2020.02	2020.02
$A(7p_{3/2})$	112.78	115.35	114.39	114.39	114.39

ture measurements. In the model we use here this magnetization is described by magnetic radius R_M and additional parameter C_S (7). Table (III) presents results of HFS calculations in DHF and DHF+RPA approximations for ^{203}Tl with different values of these parameters. Charge radius in all calculations is taken to be $R_N = 0.1306 \times 10^{-3}$ a.u. The two limiting cases are given by $R_M = 0$ and $R_M = R_N$, $C_S = 1$, which correspond to the largest and the zero nuclear contribution to the HFS radial integrals. All other results lie between these ones for both approximations. The last three columns in Table (III) correspond to three different values of R_M . Nuclear contribution grows when we decrease magnetic radius R_M and decreases with increasing parameter C_S . For each magnetic radius we choose C_S so that all five HFS constants remain constant for both approximations (!). It is particularly important because nuclear contributions for DHF and RPA approximations are very different. We can conclude that already our simple model of nuclear magnetization is degenerate and nuclear parameters R_M and C_S can not be uniquely found from atomic HFS. Consequently, there is no point in using more complex nuclear models.

V. CONCLUSIONS

In this work we propose a method for calculation hyperfine structure constants of many-electron atoms as functions of nuclear charge and magnetic radii R_N and R_M . The HFS anomaly in this method can be parametrized by b_N and b_M coefficients. If HFS anomaly is known from the experiment, then we can use coefficients b_N and b_M to determine these radii. Alternatively, we can use these coefficients to improve the accuracy for nuclear g factors of the short lived isotopes, obtained from the ratios of the HFS constants. We tested this method by calculating HFS constants of H-like thallium ion and obtained fairly good agreement with analytical

expressions from Refs. [4, 10]. Then we made calculations for neutral thallium atom described as a one-electron system. In the Dirac-Hartree-Fock approximation the ratios between hyperfine anomalies of s and $p_{1/2}$ states of neutral Tl atom and respective H-like ion are the same. However when we include spin-polarization of the core via RPA corrections, only the hyperfine anomaly for the $7s$ state remains stable. The ratios between $7s$ and $6p_{1/2}$ states change by roughly 30%, and the anomaly for the $6p_{3/2}$ state becomes very large. We conclude, that for the precision measurements of g factors it is preferable

to use the hyperfine constants for s states, while the $p_{3/2}$ states are least useful.

Acknowledgments

Thanks are due to Prof. Vladimir M. Shabaev, Prof. Ilya I. Tupitsyn and Dr. Leonid V. Skripnikov for helpful discussions. The work was supported by the Russian Foundation for Basic Research (grant # 17-02-00216).

-
- [1] A. Bohr and V. F. Weisskopf, Phys. Rev. **77**, 94 (1950).
 - [2] J. E. Rosenthal and G. Breit, Phys. Rev. **41**, 459 (1932).
 - [3] M. Crawford and A. Schawlow, Physical Review **76**, 1310 (1949).
 - [4] V. M. Shabaev, J. Phys. B **27**, 5825 (1994).
 - [5] A. Lurio and A. G. Prodell, Physical Review **101**, 79 (1956).
 - [6] D. S. Richardson, R. N. Lyman, and P. K. Majumder, Phys. Rev. A **62**, 012510 (2000).
 - [7] P. Beiersdorfer, S. B. Utter, K. L. Wong, J. R. Crespo López-Urrutia, J. A. Britten, H. Chen, C. L. Harris, R. S. Thoe, D. B. Thorn, E. Träbert, et al., Phys. Rev. A **64**, 032506 (2001).
 - [8] P. Beiersdorfer, J. Crespo López-Urrutia, S. Utter, E. Träbert, M. Gustavsson, C. Forssén, and A.-M. Mårtensson-Pendrill, **205**, 62 (2003).
 - [9] A. E. Barzakh, L. K. Batist, D. V. Fedorov, V. S. Ivanov, K. A. Mezilev, P. L. Molkanov, F. V. Moroz, S. Y. Orlov, V. N. Panteleev, and Y. M. Volkov, Phys. Rev. C **86**, 014311 (2012).
 - [10] V. M. Shabaev, M. Tomaselli, T. Kühn, A. N. Artemyev, and V. A. Yerokhin, Phys. Rev. A **56**, 252 (1997), physics/9706031.
 - [11] A.-M. Mårtensson-Pendrill, Phys. Rev. Lett. **74**, 2184 (1995).
 - [12] V. A. Dzuba, V. V. Flambaum, M. G. Kozlov, and S. G. Porsev, Sov. Phys.-JETP **87**, 885 (1998).
 - [13] M. G. Kozlov, S. G. Porsev, and W. R. Johnson, Phys. Rev. A **64**, 052107 (2001), arXiv: physics/0105090.
 - [14] M. G. H. Gustavsson, C. Forssen, and A.-M. Mårtensson-Pendrill, **127**, 347 (2000).
 - [15] M. Kozlov, S. Porsev, M. Safronova, and I. Tupitsyn, Computer Physics Communications **195**, 199 (2015), ISSN 0010-4655.
 - [16] V. F. Bratsev, G. B. Deyneka, and I. I. Tupitsyn, Bull. Acad. Sci. USSR, Phys. Ser. **41**, 173 (1977).
 - [17] S. G. Porsev, Y. G. Rakhlina, and M. G. Kozlov, J. Phys. B **32**, 1113 (1999), arXiv: physics/9810011.
 - [18] N. K. Kjølner, S. G. Porsev, P. G. Westergaard, N. Andersen, and J. W. Thomsen, Phys. Rev. A **91**, 032515 (2015).
 - [19] S. G. Porsev, M. G. Kozlov, M. S. Safronova, and I. I. Tupitsyn, Phys. Rev. A **93**, 012501 (2016), 1510.06679.
 - [20] A. P. Galván, Y. Zhao, L. Orozco, E. Gómez, A. Lange, F. Baumer, and G. Sprouse, Physics Letters B **655**, 114 (2007).